Theoretical and Applied Fracture Mechanics 84 (2016) 64–71

Contents lists available at ScienceDirect

Theoretical and Applied Fracture Mechanics

journal homepage: www.elsevier.com/locate/tafmec

High temperature fatigue behaviour in an advanced nickel based superalloy: The effects of oxidation and stress relaxation at notches

M.R. Bache [a,*], J. O'Hanlon [a], D.J. Child [b], M.C. Hardy [b]

[a] Institute of Structural Materials, Swansea University, Bay Campus, Fabian Way, Swansea SA1 8EN, United Kingdom
[b] Rolls-Royce plc, P.O. Box 31, Derby DE24 8BJ, United Kingdom

ARTICLE INFO

Article history:
Received 22 December 2015
Revised 21 March 2016
Accepted 21 March 2016
Available online 24 March 2016

ABSTRACT

The low cycle fatigue performance of the nickel based superalloy RR1000 was investigated under a variety of load waveforms at high temperature, employing a double edge notch geometry under load control. Experiments on a plain cylindrical specimen design under strain control were later performed to simulate the constrained conditions at the root of the notch in order to characterise the interaction between surface constituents and the environment. A significant fatigue debit was demonstrated under both load/strain scenarios when superimposing a dwell period at the minimum point of the cycle. This debit was attributed to a reduction in fatigue crack initiation life resulting from oxidation damage which subsequently cracks under cyclic tension together with a modification to the mean stress through cyclic stabilisation. The same dwell period superimposed at the peak of the cycle was essentially benign for excursions under strain control loading.

1. Introduction

The most critically stressed features in engineering components will invariably be associated with notches. With reference to aero-engine compressor and turbine disc components, such macroscopic notch geometries may take a wide variety of forms, ranging from through section holes utilised for cooling or mechanical assembly to fir tree aerofoil attachments, with elastic stress concentration factors typically falling within the range of $2 \leqslant K_t \leqslant 5$. Understanding material behaviour at the root of these features under representative combinations of stress, temperature and environment is crucial to the design and lifing of these safety–critical rotating parts.

Although recognising that service components will experience a complex combination of these controlling parameters, in the first instance, laboratory assessments to develop such understanding will be normally be based on constant amplitude (baseline) fatigue experiments under isothermal and stable environmental conditions, usually in atmospheric air. However, a common approach towards more representative conditions is to include slightly more complex loading waveforms through the use of dwell periods, simulating the superposition of static loading (creep effects), constantly being mindful of the coincident, additional time of exposure to aggressive species, e.g. the role of oxidation.

In the case of advanced nickel based superalloys, fatigue endurance behaviour from dwell periods at maximum load or strain (referred to here as peak dwell fatigue) has been widely reported in the past. More recently, however, the contrasting scenario of minimum dwell fatigue, i.e. a dwell period imposed at minimum load or strain within the cycle, has received increasing interest due to its association to out-of-phase thermo-mechanical fatigue behaviour (OOP TMF). Bache [1,2] and the team including Gabb and Telesman and their respective co-workers [3–5], have reported large reductions in fatigue life under minimum dwell in contrast to peak dwell and baseline fatigue cycling, along with high levels of environmental interaction at temperatures between 650 °C and 704 °C. All of these studies have focussed on the behaviour of constrained notch specimens under uniaxial loading. Whilst implicating both the effects of oxidation and plasticity within the notches as controlling factors behind performance, the partitioning of these separate effects has not been fully quantified.

This paper will summarise our previously reported notch data that demonstrates the marked effect of minimum dwell fatigue on the fatigue response of the nickel-based superalloy RR1000 at 650 °C [1,2] in addition to more recent fatigue experiments conducted on plain specimens in order to simulate and model the constrained conditions experienced at the root of the notch. The previous lack of fatigue debit measured in notch specimens when comparing peak dwell to baseline loading scenarios suggested that any adverse effects of creep damage development within the notches during periods of peak dwell loading and any coincident

* Corresponding author.
E-mail address: m.r.bache@swansea.ac.uk (M.R. Bache).

http://dx.doi.org/10.1016/j.tafmec.2016.03.007
0167-8442/

Nomenclature

ε_{min}	minimum strain applied during strain control fatigue cycle (%)	P_{min}	minimum applied load during load control fatigue cycle (kN)
ε_{max}	maximum strain applied during strain control fatigue cycle (%)	P_{max}	maximum applied load during load control fatigue cycle (kN)
K_t	fatigue stress concentration factor	R_a	surface roughness average (μm)
N_i	number of cycles to crack initiation (defined by DCPD response)	V	voltage measured across notch using pulsed potential drop technique (V)
N_f	number of cycles to failure		

adverse effects of oxidation are offset by stress relaxation reducing the effective mean stress under positive R ratio cycles. In the specific case of creep, it was presumed that the elastic constraint surrounding the critically stressed material at the root of the notch significantly resisted creep strain accumulation. It should be re-emphasised that the minimum dwell phenomenon was dominated by the effects on initiation life measured in the notch specimens rather than significantly affecting damage tolerance characteristics. The recent design of experiments for plain specimens was intended to explore the complimentary effects of oxidation and constitutive behaviour by definition of the stress–strain loop response and detailed characterisation of crack initiation mechanisms under the oxidising environment.

2. Experimental methods

The nominal composition of the nickel disc alloy RR1000 is provided in Table 1.

All notched and plain laboratory scale fatigue specimens were machined from a RR1000 disc rotor forging that had been processed and heat treated to a standard proprietary condition. Details concerning the chemical composition, typical microstructures and basic mechanical properties of polycrystalline RR1000 have been previously reported [6–9]. The current material contained approximately 47% of precipitation phases (a combination of primary, secondary and tertiary γ') within a FCC matrix. Incoherent grain boundary primary γ' particles that are 1–5 μm in size control the grain size of the alloy, in this case to an average size of ASTM 13-11 (4–8 μm). The typical microstructure is illustrated in Fig. 1.

The double edge notch specimen design is illustrated in Fig. 2. Each semi-circular notch provides an average, elastic stress concentration factor of $K_t = 1.9$ along the notch root, representative of moderate stress raising component features. The notches were machined using an end milling technique with all edges deburred. Unless specified, the notches in all specimens were subsequently etched (to simulate component inspection preparation) and shot peened to a proprietary standard.

Plain round bar test pieces were machined, low stress ground and longitudinally polished to produce a high quality surface finish ($R_a < 0.25$ μm) to minimise surface initiating features and to minimise residual stresses, Fig. 3.

Three distinct waveforms were employed under load control throughout the course of the notch testing matrix. "Baseline" cyclic loading applied a trapezoidal, 15 cycle per minute waveform consisting of 1 s linear rise and fall ramps with 1 s holds at peak and minimum load (designated 1/1/1/1). The "peak load dwell" cycle comprised similar rise, fall and minimum load periods but incorporated a hold at peak load for 10 s (1/10/1/1). In contrast, "minimum load dwell" applied the 10 s dwell at the minimum load condition

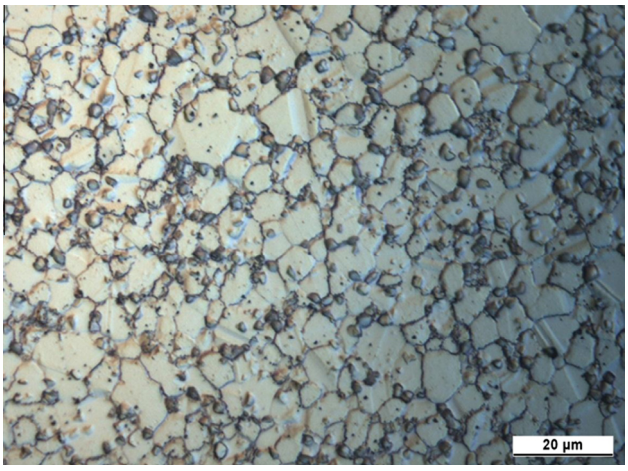

Fig. 1. Typical microstructure of Fine Grained RR1000.

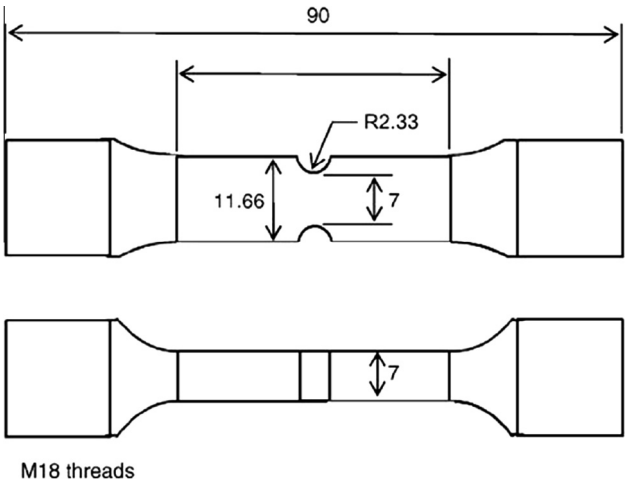

Fig. 2. Double edge notch specimen geometry (dimensions in mm).

Table 1
RR1000 nominal composition (wt%).

RR1000	Co	Cr	Mo	Ti	Al	Ta	Hf	Zr	C	B	Ni
	18.5	15	5	3.6	3	2	0.5	0.06	0.027	0.015	Balance

Fig. 3. Plain round bar specimen.

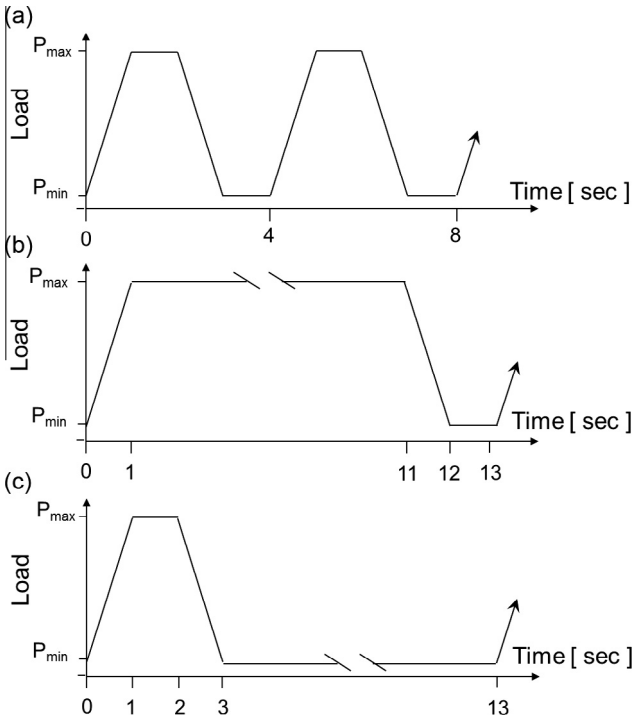

Fig. 4. Applied waveforms; (a) 1/1/1/1 baseline, (b) 1/10/1/1 peak load dwell and (c) 1/1/1/10 minimum load dwell.

(1/1/1/10). The waveforms are represented schematically in Fig. 4. An applied stress ratio of 0.01 was employed throughout this series of tests. These load control LCF tests employed the best practise described within a relevant standard procedure [10].

Data are presented for tests performed at 650 °C employing various servo-hydraulic or servo-mechanical test machines equipped with radiant furnaces. Specimen temperatures were monitored using calibrated type *N* thermocouples.

With particular respect to the notch specimens, it was intended from the outset that the investigation would concentrate on a single peak load/stress condition, specifically, that necessary to induce baseline fatigue failures in approximately 30,000 cycles in laboratory air. This order of cyclic life is typically employed for the design of compressor and turbine discs. Prior knowledge of RR1000 elevated temperature fatigue performance and an initial series of scoping tests then helped to define this specific stress level. Although this parameter is deemed as proprietary information, this does not detract from the trends in performance and mechanistic studies described in the present paper. Ultimately, as a result of the various applied waveforms, specimen failures were induced over a range of life from 10^3 to 10^5 cycles.

Table 2
Test conditions applied to notch specimens.

Waveform	Environment
1/1/1/1	Air
1/10/1/1	Air
1/1/1/10	Air
1/1/1/1	Vacuum (10^{-5} mbar)

The notch fatigue tests were repeated (usually a minimum of three per condition) employing the various forms of loading waveform in either laboratory air or vacuum (10^{-5} mbar) environments. A summary of the fatigue test conditions is given in Table 2. Direct current potential drop measurements were taken at regular predetermined intervals, employing a pulsed 30 A current supply and diagonally opposed measurement probes welded across each specimen notch. This was in order to define an initiation life, N_i, for each test in addition to the total life to failure, N_f, as defined by complete specimen rupture. The criterion for crack initiation was set after retrospective inspection of all voltage-cycles data from the individual tests and a nominal increment in notch voltage of 25 μV over the normalised stable voltage measured prior to cracking was employed.

Plain cylindrical specimens were tested in air under constant amplitude strain control, at the peak strain condition of 0.7%. The baseline 1/1/1/1 trapezoidal and a 1/1/1/30 minimum dwell waveform were employed, with the strain ratio set at zero (i.e. cycling between zero and maximum strain values). Strain was controlled employing a commercial, side sprung strain gauge bridge extensometer as described in a relevant standard procedure [11]. One further specimen was tested under strain control at a peak strain level of 0.9%. The evolution of peak stress per cycle measured from this latter test was used to define the stabilised peak stress condition at the "half-life" stage [11]. This peak stress value was then applied under load control to all remaining plain specimens. The intention throughout the plain cylindrical test matrix was to generate fatigue fractures across a similar range of lives as measured in the notch specimens.

All fractured specimens were inspected using optical and scanning electron microscopy to identify the number and location of crack initiation sites and confirm the dominant mechanisms controlling crack initiation and growth. Energy dispersive X-ray inspection (EDX) was employed to identify the elemental composition of surface features.

3. Results

The endurance data relating to the notch fatigue experiments conducted at 650 °C are reproduced in the cumulative frequency plot in Fig. 5. The baseline and peak load dwell data from tests conducted in air correlate well, indicating no significant effect of the extended dwell period at the maximum load condition. Data generated under a vacuum of 10^{-5} mbar indicated a moderately stron-

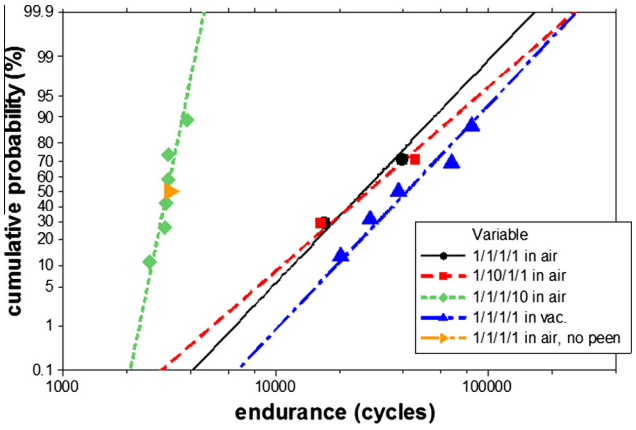

Fig. 5. Endurance data for notch fatigue experiments plotted in terms of cumulative frequency [1].

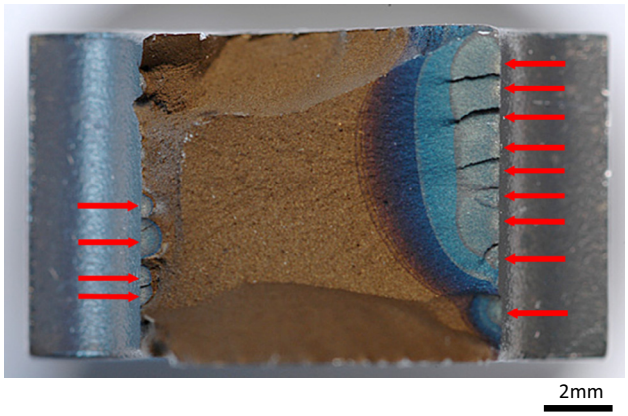

Fig. 6. Typical example of multiple crack initiation in a double edge notch specimen tested under the minimum load dwell waveform in air at 650 °C (individual initiation sites indicated by arrows).

ger fatigue performance. The most striking effect amongst the entire dataset, however, was the notable reduction in fatigue strength under the waveform incorporating the dwell at minimum load, with reductions in fatigue life of approximately one order of magnitude compared to the combined baseline and peak load dwell experiments.

Distinct differences were also noted in the form of fatigue crack initiation and growth to fracture. Under the minimum load dwell waveform, multiple cracks initiated along the root of either notch in all specimens, for example at least thirteen individual cracks are identified in Fig. 6. Obviously, the progressive oxidation of these cracks due to exposure to air at 650 °C has helped define these features through oxide tinting. Alternatively, notch specimens tested either under the baseline or the maximum dwell waveform rarely initiated cracking from more than three isolated sites.

The effect of the minimum load dwell on crack initiation life is exemplified by the potential drop data illustrated in Fig. 7. With both tests conducted at an identical stress level, the minimum load dwell test has clearly initiated cracking relatively early. Allowing for the degree of sensitivity of the PD monitoring across the 3 mm radius notch, when comparing the initial stages of crack growth in the two examples this appears to be slightly more gradual under baseline cycling, whilst the slopes to the *V*/*N* curves in the stages immediately prior to fracture seem to be very similar. It can be confirmed, therefore, that the greatest influence on fatigue life from the different waveforms is dominated by initiation behaviour, not changes to the damage tolerance characteristics.

Switching attention to the plain cylindrical specimens and concentrating alone on the baseline and minimum load waveforms, Fig. 8 illustrates the endurance data for the constant amplitude strain control tests conducted at 0.7% peak strain, again represented by cumulative frequency. The total time on test whilst exposed to air at elevated temperature is indicated for each specimen. Fig. 9 then plots data from the one strain control test conducted at 0.9% peak strain (represented by the data point with a total exposure time of 27.5 h) and the associated load control tests performed at the stabilised peak stress condition previously defined by that single strain control test. As noted from the notch data, the minimum load dwell waveform consistently induces a significantly weaker fatigue performance of a similar order of magnitude. Note that the levels of strain and the resultant stabilised stress conditions selected have generated fatigue failures across a range of lives similar to those found in the notch experiments.

Fractography of the plain specimens highlighted the importance of oxidation in controlling crack initiation and early stage propagation. The example presented in Fig. 10 was taken from the specimen tested under strain control at 0.9% peak strain and minimum dwell waveform which survived for the longest cyclic life and therefore longest exposed time period (8060 cycles, approximately 74 h). Crack initiation was defined from at least ten sites around the periphery of the specimen on different planes along the gauge length. Higher magnification images of the individual sites, for example Fig. 11, indicated cracks initiate from very shallow, rough, pit like features. Planar transgranular fracture extends inwards from the surface for approximately 30 μm then transferring to a mixed mode and later an intergranular form. Remote from the eventual plane of fracture, multiple cracks were found often associated with oxide nodules residing on the gauge surface, Fig. 12, with clear signs of oxidation built up along the flanks of these sub-critical cracks, Fig. 13.

4. Discussion

Our original investigation into the effects of dwell loading on the fatigue performance of the advanced nickel based superalloy RR1000 [1,2], employing a double edge notched specimen geometry, proved to be consistent with contemporary notch fatigue studies of alternative disc alloys [3–5]. The adverse response to dwell

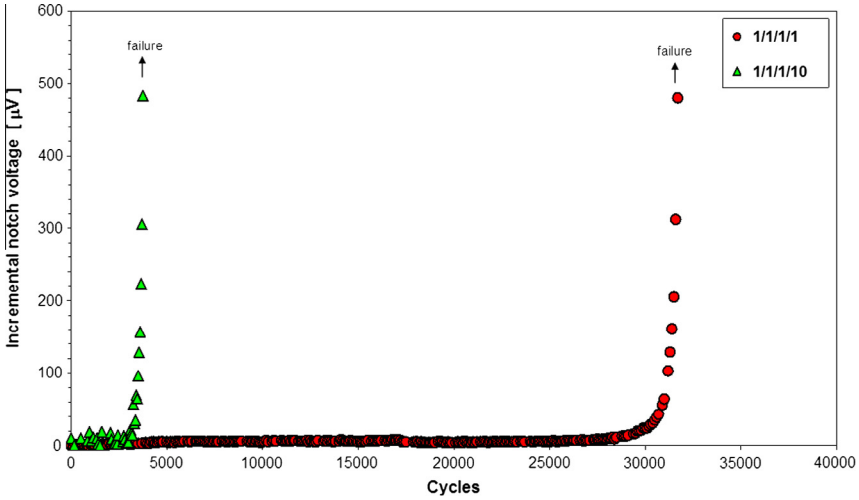

Fig. 7. Crack initiation and growth monitored in notch specimens under different waveforms.

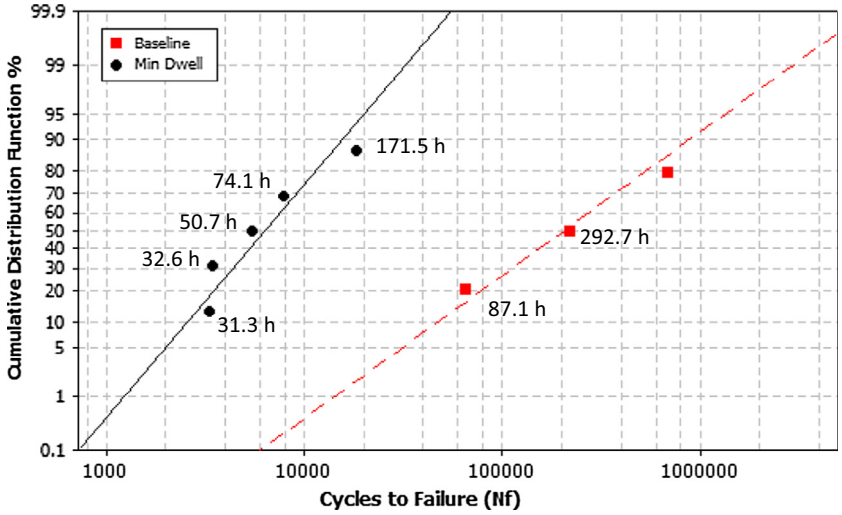

Fig. 8. Endurance data for plain cylindrical specimens tested under strain control at 0.7%, $R = 0$, plotted in terms of cumulative frequency (associated exposure times indicated in hours).

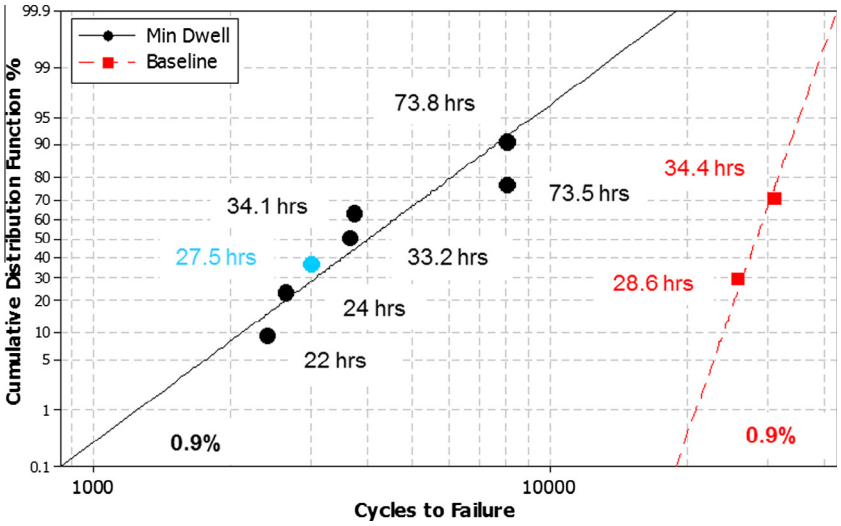

Fig. 9. Endurance data for plain cylindrical specimens tested at the stabilised stress level measured from the single strain control test conducted at 0.9%, $R = 0$, plotted in terms of cumulative frequency (associated exposure times indicated in hours).

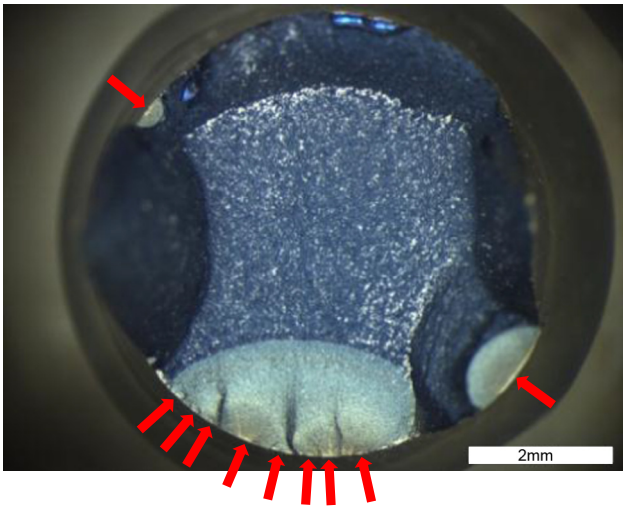

Fig. 10. Crack initiation in a round bar specimen, $\varepsilon_{max} = 0.9\%$, $R = 0$ (individual initiation sites indicated by arrows).

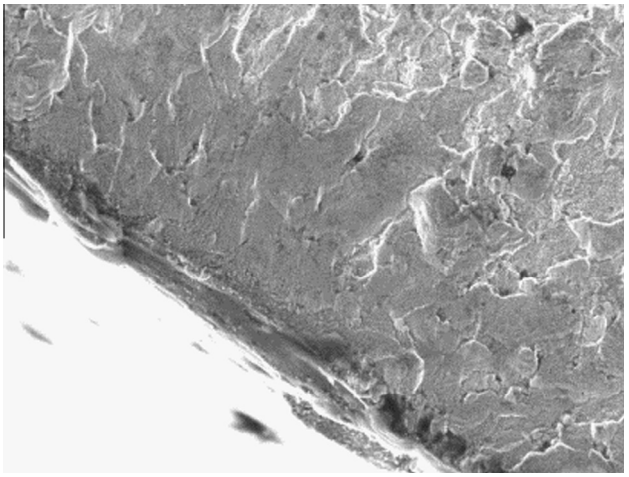

Fig. 11. Crack initiation and early stages of growth.

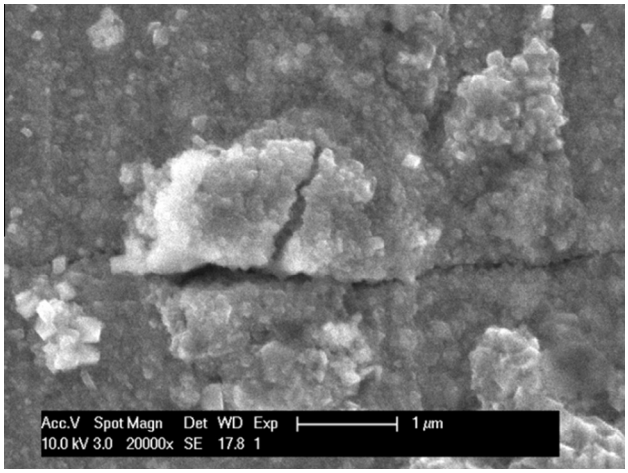

Fig. 12. Crack initiation from surface oxide nodule.

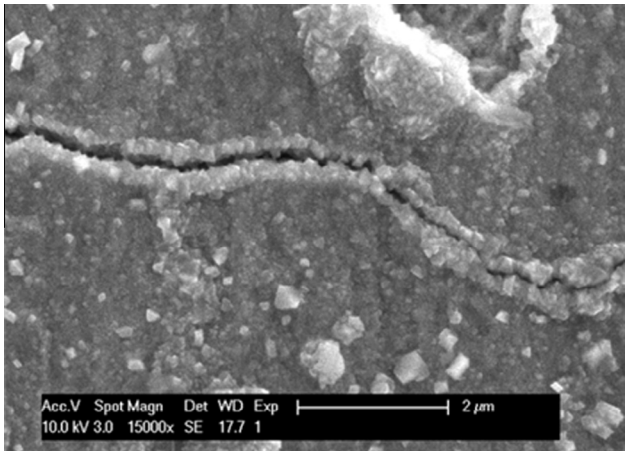

Fig. 13. Oxidation along flanks of a sub-critical crack.

imposed at the minimum point of the load cycle in combination with exposure to air at high temperature is now accepted as a true mechanical phenomenon. However, prior to the present study the complex interaction between cyclic stress (or strain) and the environment had not been fully characterised.

When previously referring to the notch LCF data represented in Fig. 5, it was proposed that the marked reduction in fatigue strength noted under minimum dwell cycling was due to cyclic damage initiating failures under tensile applied stress following oxidation of the surface at the notch root. In contrast, it was believed that oxidation damage that is produced during peak load dwells would resist cracking under localised compression during the subsequent unloading half cycle. It was pertinent to note that the strongest performance during the entire notch assessment was measured under relatively hard vacuum.

The employment of plain cylindrical specimens subjected to either strain controlled cycles, simulating the constraint experienced by the critically stressed volume of material at the notch roots, or load controlled cycles have assisted in identifying the role of oxidation on early fatigue crack initiation. Specific to the RR1000 alloy under investigation, Fig. 12 demonstrates the prevalence of relatively brittle oxide nodules which form on surface breaking grain boundaries and subsequently fracture under the applied tensile half-cycle. Preferential oxidation along the flanks of the early stage crack, Fig. 13, may infer modifications to the rate of crack growth in this stage, however, any effects would have been too

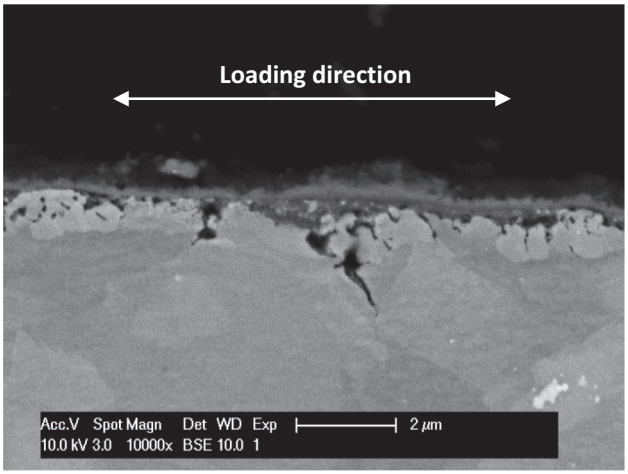

Fig. 14. Surface oxidation and transgranular alumina ingress.

subtle to monitor during the pulsed DCPD monitoring of the notch experiments. Instead, those tests clearly identified the generic effects of early initiation, Fig. 7, with the period spent during sub-critical crack growth being relatively short under all circumstances. The fracture mode quickly transfers from transgranular to mixed mode (Fig. 11) and onwards to intergranular as a result of the stress assisted grain boundary oxidation (SAGBO) mechanism that predominates high temperature fatigue crack behaviour

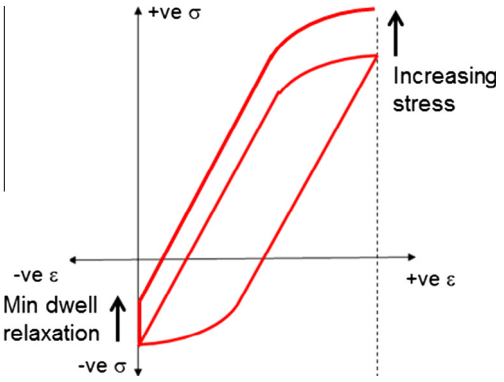

Fig. 15. Increase in mean stress imposed at the notch root through relaxation during the minimum dwell period.

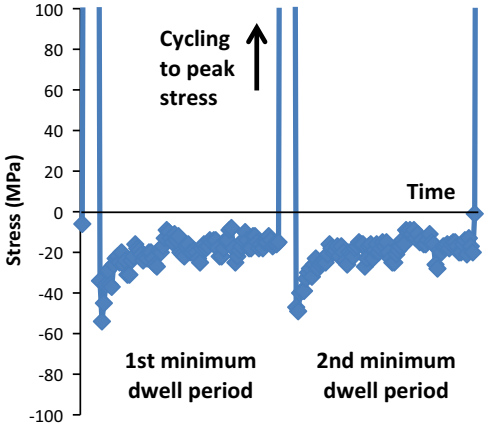

Fig. 16. Stress relaxation during the initial two cycles of a strain controlled LCF test conducted with a minimum dwell waveform.

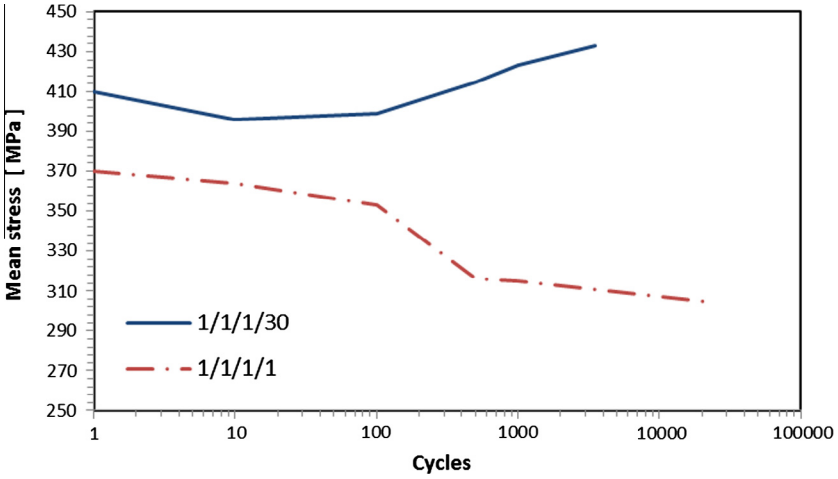

Fig. 17. Evolution of mean stress during strain control fatigue, under baseline and minimum dwell waveforms.

under creep-fatigue regimes in this specific alloy [12]. However, during the earliest stages of cracking, Fig. 14, oxidation can also promote the ingress of alumina "fingers" on transgranular planes, also reported by Foss et al. [13]. The mechanisms of oxide formation and the associated role of applied stress, whether static or cyclic, is an area of ongoing interest.

It was encouraging to find that through careful consideration of the applied strain conditions very similar magnitudes of fatigue debit were induced in the plain specimens to that previously reported for our notch experiments. The plain specimens also demonstrated the multiple instances of crack initiation sites previously noted at the root of the notch specimens.

Although it appears that the interaction of material microstructure and the environment is affecting the high temperature performance of the notch specimens, a secondary potent driver behind the response may be the associated stress relaxation occurring at the notch root. Despite testing under load control, due to the local constraint, under the nominal zero to maximum baseline LCF cycle the peak and minimum stress induced within the critically stressed volume will both fall with continuous cycling, leading to a reducing mean stress throughout each individual test. The rate of this relaxation will be enhanced by the superposition of a dwell period at the peak of the cycle, i.e. a form of creep interaction effectively offering a benefit to fatigue performance. In contrast, the mean applied stress will increase as a result of dwell at the minimum point in the cycle, as represented schematically in Fig. 15, promoting early crack initiation and raising the peak crack driving force. Constitutive loop information measured from the first two cycles of a strain controlled, minimum dwell LCF test on a plain cylindrical specimen illustrates this effect by focussing on the minimum stress as a function of time, Fig. 16. The combined effects on the peak and minimum stresses are plotted as the resultant mean stress versus cycles in Fig. 17. Whereas a specimen continuously softens when a baseline cycle is applied, after approximately 100 strain cycles the mean stress significantly increases throughout the remaining life under the minimum dwell waveform.

The minimum dwell phenomenon described during these limited studies warrants further consideration in support of engineering design and component life prediction. The characterisation of notch fatigue behaviour offers an instructive test technique for the evaluation of this complex interaction between stress state, material microstructure and an aggressive environment.

5. Conclusions

The following high level conclusions are drawn from the present research:

- A life debit is induced in the nickel based superalloy RR1000 by superimposing a dwell period at the minimum point of the fatigue cycle under elevated temperature in an oxidising environment.
- Dwell loading at the peak of the cycle is effectively benign.
- The formation of oxide nodules at surface breaking grain boundaries promotes early crack initiation under the minimum dwell conditions.
- The stress concentration effects at notches were successfully replicated through the employment of plain cylindrical specimens under strain control LCF.

Acknowledgements

The notch fatigue data in this paper were originally generated in the MACE (Materials for Arduous Cycles and Emissions) Project (TP/2/ET/6/I/10037), funded by the Technology Strategy Board (formerly Department of Trade and Industry). The recent research utilising plain cylindrical specimens was part funded by the EPSRC Rolls-Royce Strategic Partnership in Structural Metallic Systems for Gas Turbines (grants EP/H500383/1 and EP/H022309/1). The provision of materials and technical support from Rolls-Royce plc is gratefully acknowledged.

References

[1] M.R. Bache, J.P. Jones, G.L. Drew, M.C. Hardy, N. Fox, Environment and time dependent effects on the fatigue response of an advanced nickel based superalloy, Int. J. Fatigue 31 (2009) 1719–1723.
[2] M.R. Bache, W.J. Evans, M.C. Hardy, The effects of environment and loading waveform on fatigue crack growth in Inconel 718, Int. J. Fatigue 21 (1999). S69–S77.
[3] J. Telesman, T.P. Gabb, Y. Yamada, L.J. Ghosn, D. Hornbach, N. Jayaraman, Dwell notch low cycle fatigue behaviour of a powder metallurgy nickel disk alloy, in: Superalloys 2012, 2012, pp. 853–862.
[4] T.P. Gabb, J. Telesman, P.T. Kantzos, J.W. Smith, P.F. Browning, Effects of high temperature exposure on fatigue life of disk superalloys, in: K.A. Green (Ed.), Superalloys 2004, TMS (The Minerals, Metals & Materials Society), Warrendale, PA, USA, 2004, pp. 269–274.

[5] J. Telesman, T.P. Gabb, L.J. Ghosn, J. Gayda Jr., Effect of Notches on Creep-Fatigue Behaviour of a P/M Nickel-Based Superalloy, NASA/TM-2015-218887, 2015.
[6] M.C. Hardy, B. Zirbel, G. Shen, R. Shankar, Developing damage tolerance and creep resistance in a high strength nickel alloy for disc applications, in: K.A. Green et al. (Eds.), Superalloys 2004, TMS (The Minerals, Metals & Materials Society), Warrendale, PA, USA, 2004, pp. 83–90.
[7] H.T. Pang, P.A.S. Reed, Fatigue crack initiation and short crack growth in nickel base turbine disc alloys – the effects of microstructure and operating parameters, Int. J. Fatigue 25 (2003) 1089–1099.
[8] D. Turan, D. Hunt, D.M. Knowles, Dwell time effect on fatigue crack growth of RR1000 superalloy, Mater. Sci. Technol. 23 (2) (2007) 183–188.
[9] S. Everitt, M.J. Starink, H.T. Pang, I.M. Wilcock, M.B. Henderson, P.A.S. Reed, A comparison of high temperature fatigue crack propagation in various subsolvus heat treated turbine disc alloys, Mater. Sci. Technol. 23 (12) (2007) 1419–1423.
[10] BS EN 6072:2010, Aerospace Series, Metallic Materials, Test Methods, Constant Amplitude Fatigue Testing, British Standards Institution, 2010.
[11] BS 7270:1990, Method for Constant Amplitude Strain Controlled Fatigue Testing, British Standards Institution, 1990.
[12] H.Y. Li, J.F. Sun, M.C. Hardy, H.E. Evans, S.J. Williams, T.J.A. Doel, P. Bowen, Effects of microstructure on high temperature dwell fatigue crack growth in a coarse grain PM nickel based superalloy, Acta Mater. 90 (2015) 355–369.
[13] B.J. Foss, M.C. Hardy, D.J. Child, D.S. McPhail, B.A. Shollock, Oxidation of a commercial nickel-based superalloy under static loading, JOM 66 (12) (2014) 2516–2524.